

# Surface properties of $\text{CaNi}_5$ hydrogen storage alloy

M. P. SRIDHAR KUMAR, B. VISWANATHAN, C. S. SWAMY, V. SRINIVASAN  
*Department of Chemistry, Indian Institute of Technology, Madras 600 036, India*

The Ca 2p, Ni 2p and O 1s emissions of the air-exposed sample of  $\text{CaNi}_5$  indicate that all the calcium and most of the nickel are present in the oxidized state. Interestingly, it is observed that all the peaks are shifted by 3 to 4 eV towards higher binding energy values. This observation has been attributed to the presence of insulating oxide phases leading to partial charging of the sample during the experiment. Depth profiling by argon-ion sputtering removes the insulating oxide species and the sample etched for 7300 sec shows the presence of metallic nickel and mostly metallic calcium. XPS analysis indicates that preferential segregation of calcium in the  $\text{CaNi}_5$  alloy is mainly due to induced surface reaction with oxygen.

## 1. Introduction

It is known that intermetallics used for hydrogen storage purposes require special activation procedures [1-5]. The activation procedures adopted for the intermetallics, their chemical reactivity towards the atmosphere, as well as their amenability for activation under various pretreatment conditions, have been reported [6]. Normally most of the intermetallics, in the as-received condition, form surface oxides and hydroxides, the relative amount of these species being dependent upon the nature of the alloys. In order to devise suitable activation procedures, it is necessary that the nature of the surface species formed is identified precisely and the extent of these species estimated so as to evolve the activation procedures.

In addition, the reactivity of the constituent elements could lead to preferential accumulation of one of the species on the surface (segregation) as compared to the bulk composition. The increased concentration of one of the constituents of the intermetallics at the surface could arise out of various factors such as differences in the surface energies of the elements, the chemical reaction-induced segregation, release of strain energy or other entropy factors.

Among the various  $\text{AB}_5$ -type alloys, the surface properties of  $\text{LaNi}_5$  and  $\text{ThNi}_5$  have been examined by Schlapbach and Brundle [7] by the XPS technique. They have shown that lanthanum or thorium is segregated to the surface when  $\text{LaNi}_5$  or  $\text{ThNi}_5$  is exposed to increasing doses of oxygen, this chemisorption-induced segregation being stronger in  $\text{LaNi}_5$  compared to  $\text{ThNi}_5$ . Schlapbach [8] has shown that lanthanum is preferentially oxidized when  $\text{LaNi}_5$  is exposed to oxygen. Other studies propose that both compounds may yield oxides and hydroxides on exposure to the atmosphere [9]. In view of these reports, it was considered worthwhile to investigate a related system, namely  $\text{CaNi}_5$  to answer the following questions.

(i) In this  $\text{AB}_5$ -type compound, if one of the components, namely calcium, were to segregate to the surface, then what is the driving force for this segregation?

(ii) What are the major surface species present on the as-received sample, i.e. the sample exposed to the atmosphere?

(iii) What is the depth profile of these surface species?

(iv) Knowing the nature of the surface species, how can a suitable activation procedure for this intermetallic compound be devised?

(v) How do the results obtained with the  $\text{CaNi}_5$  system compare with those reported for other  $\text{AB}_5$ -type systems, such as  $\text{LaNi}_5$  and  $\text{ThNi}_5$ ?

## 2. Experimental details

The  $\text{CaNi}_5$  alloy (HYSTOR-201) of MPD Technology Corporation, New Jersey, USA, was used for the studies. The commercial sample was powdered in air, pressed into a pellet and used for the measurements.

XPS data were obtained with a VG Scientific Ltd UK ESCALAB Mark II instrument. The X-ray source used for XPS was a magnesium anode ( $\text{MgK}_\alpha$ , 1253.6 eV) with 50 eV pass energy. The surface was cleaned by argon-ion bombardment and was subsequently exposed to increasing doses of oxygen in the preparation chamber.

For the XPS measurements, the samples were subjected to argon-ion sputtering at  $5 \times 10^{-5}$  m bar with beam voltages of 8 keV and 40  $\mu\text{A}$  of filament current. The XPS spectra obtained were stored and processed using an Apple II Europlus microcomputer. All the measurements were carried out at room temperature. The elemental atomic ratios were derived from the peak intensities and photoionization cross-sections. The C 1s line at 284.8 eV was used as the binding energy reference and the Ni 2p, Ca 2p, Ca 2s, O 1s and C 1s regions were scanned.

## 3. Results and discussion

Core level emissions of Ca (2s and 2p), Ni (2p), O (1s) and C (1s) were monitored using  $\text{MgK}_\alpha$  radiation with the as-received sample and the sample sputtered with argon ions for different time periods. The experimental spectra obtained for Ca 2p, Ni 2p, O 1s and C 1s are

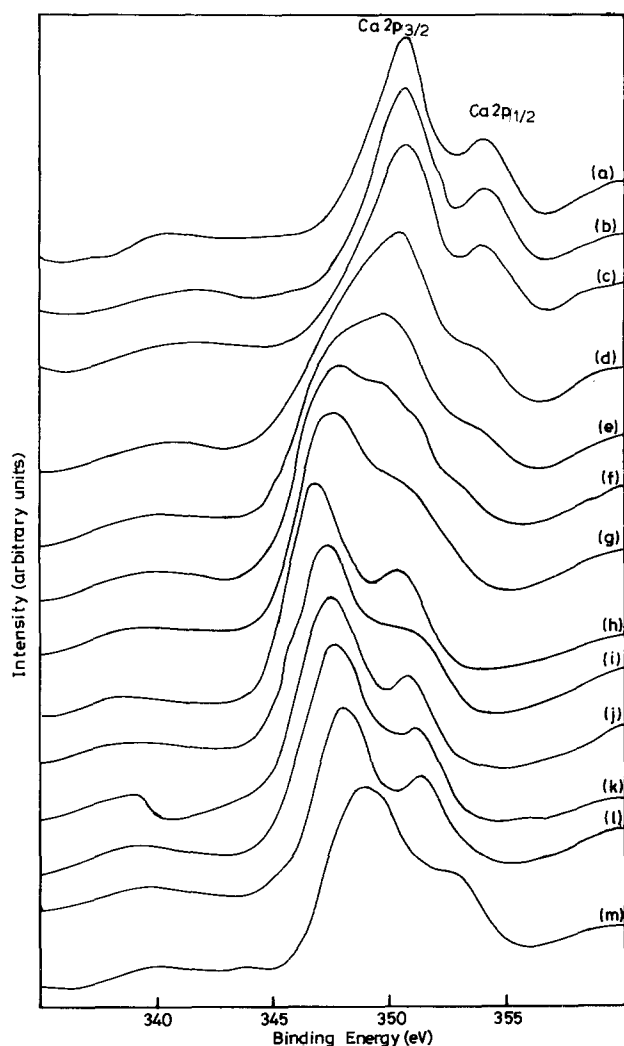


Figure 1 XPS (Ca 2p) spectra for the as-received, argon-ion sputtered and oxygen-exposed sample of the  $\text{CaNi}_5$  alloy; (a) as-received, (b) to (h) sputtered for 45, 165, 400, 1000, 1900, 3700 and 7300 sec, respectively, (i) to (l) exposed to oxygen at  $10^{-5}$  torr for 10 sec,  $10^{-4}$  torr for 20 min, 100 torr for 20 min and 0.4 atm for 22 h, respectively, (m) air-exposed (in a desiccator for 30 d).

given in Figs 1 to 4, respectively. These figures also include the XP spectra obtained with the fully etched sample exposed to different doses of oxygen. The information extracted from these spectra, namely the observed binding energies of the various core levels, are summarized in Table I.

The Ca 2s and 2p spectra obtained with the sample etched for 7300 sec show binding energy values of 438.7 (2s), 346.8 ( $2p_{3/2}$ ) and 350.3 ( $2p_{1/2}$ ) eV (see Fig. 1h). The values closely correspond to the binding energy values reported [10] for metallic calcium in zero valance state. The O 1s peak at 530.0 eV could arise out of residual adsorbed oxygen species. The C 1s peak at 284.8 eV might be from the residual carbon from the pump oil and has been used as reference. However, the other peak at 291.2 eV, together with the O 1s peak is 532.1 eV could have arisen from the carbonate species formed as a result of the interaction of  $\text{CO}_2$  in the atmosphere with surface nickel species.

In comparison to this, the as-received sample gives rise to Ca 2s and 2p emissions at higher binding energy values, namely at 442.3 (2s), 350.9 ( $2p_{3/2}$ ) and 354.2 ( $2p_{1/2}$ ) eV. It is evident that calcium on the surface of the as-received sample is in the oxidized form. However, the high binding energy values observed might be due to partial charging of the sample. This aspect is also exemplified by the shift of the O 1s as well as Ni 2p peaks to higher binding energy values as compared to the normal values observed for oxide and  $\text{Ni}^{2+}$  ions. Though this partial charging of the sample shifts the emissions to higher binding energy values, the characteristics of these emissions could be deduced from chemical intuition as well as the characteristic nature of these peaks. In the as-received sample, the Ni  $2p_{3/2}$  line spans a broad range converting from the metallic state at 853.0 eV to nearly 870 eV, inclusive of any possible satellite features. This broad feature, which can arise due to

TABLE I XPS data for the  $\text{CaNi}_5$  alloy

Sample	Binding energy (eV)											
	C 1s		Ca 2s*	Ca 2p*		Ni 2p		O 1s				
				$2p_{3/2}$	$2p_{1/2}$	$2p_{3/2}$	$2p_{1/2}$					
Sputted (sec)												
0 <sup>†</sup>	248.8	288.6	293.0	442.3	350.9	354.2	860.2	878.0	878.0	535.0		
45	284.9	288.4	293.2	442.2	350.8	354.1	859.0	878.0	878.0	535.0		
165	284.9	289.1	293.1	441.4	350.7	354.0	859.2	877.8	877.8	535.3		
400	284.8		292.6		350.5	353.9	852.8	870.4	874.0	534.3		
1000	284.8		291.3	440.6	349.7		852.9	870.5	874.0	532.7		
1900	284.8		291.2		347.7		852.9	870.3		532.7		
3700	284.8	–	291.2	439.8	347.6		853.0	870.3		532.5		
5500									530.3	532.3		
7300	284.8	–	291.2	438.7	346.8	350.3	853.0	–	870.3	–	530.0	532.1
Exposed to oxygen (torr)												
$10^{-5}$ for 10 sec	284.8	–	290.7	439.3	347.3	350.7	853.0		870.2		531.8	
$10^{-4}$ for 20 min	284.9	–	290.9	439.3	347.5	350.9	853.0		870.2		531.6	
100 for 20 min	285.0		290.5	439.5	347.7	351.2	853.0		870.2		531.9	
300 for 22 h	285.0		290.5	440.0	348.0	351.3	853.0		870.2		532.0	
Air-exposed <sup>‡</sup>	285.2		290.5	440.4	349.0		853.2	857.0	874.4		532.8	

\*Refers only to the peak maximum obtained. The peaks are broad and are further deconvoluted for identification purposes.

<sup>†</sup>As-received sample.

<sup>‡</sup>Exposed to air in a desiccator for 30 d.

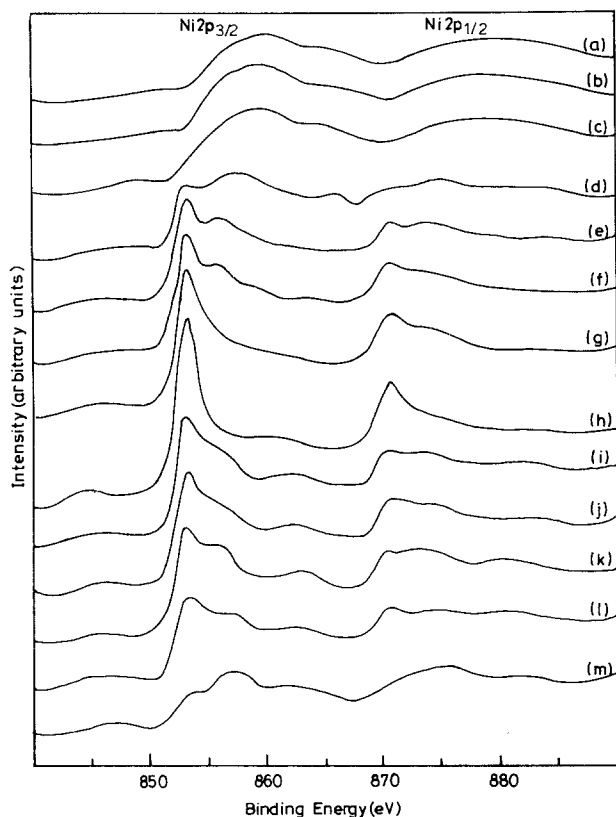


Figure 2 XPS (Ni 2p) spectra for the  $\text{CaNi}_5$  alloy; (a) to (m) as in Fig. 1.

the presence of multiple valance states (in this case  $\text{Ni(O)}$ ,  $\text{Ni}^{2+}$  and  $\text{Ni}^{3+}$ ) and the attendant satellite emissions, indicates the presence of the  $\text{Ni(O)}$ ,  $\text{Ni}^{2+}$  and  $\text{Ni}^{3+}$  states on the surface. The additional C 1s features observed at 288.6 and 293.0 eV could have arisen from the interaction of  $\text{CO}_2$  from the atmosphere with the oxidized metallic surfaces [11]. This also accounts for the broad O 1s emission, indicating that in addition to the oxide oxygen with emissions around 530 eV, other types of oxygenated species resulting from carbonate type, adsorbed  $\text{CO}_2$  type as well as carboxyl oxygen type species are present on the surface.

The validity of these assignments can also be ascertained from emissions obtained for the same core levels as a result of exposure of the fully sputtered sample to various doses of oxygen. The oxygen exposure progressively increased the formation of  $\text{CaO}$  and  $\text{Ni}^{2+}$  species as is evident from the Ni 2p emission around 855 eV. The presence of oxidic species of nickel is evident from the satellite feature at 862 eV. However, it should be remarked that complete oxidation of all the nickel species on the surface is not realized as the Ni 2p emission is observed around 853 eV even in the samples exposed to oxygen for a considerable length of time. In case of  $\text{LaNi}_5$  it is observed that lanthanum on the surface is preferentially oxidized, while the surface nickel is not oxidized [7]. Although this is not completely true in the case of the  $\text{CaNi}_5$  system, preferential oxidation of calcium is observed together with partial oxidation of nickel. This peculiar behaviour of this system, similar to other  $\text{AB}_5$ -type systems, may be responsible for the facile dissociative adsorption of hydrogen, which could be

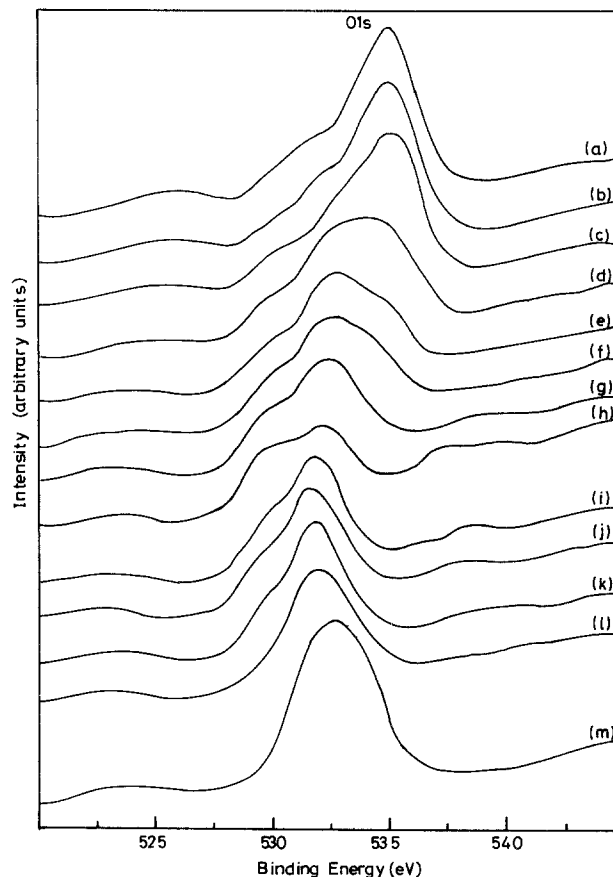


Figure 3 XPS (O 1s) spectra for the  $\text{CaNi}_5$  alloy; (a) to (m) as in Fig. 1.

used for activating this intermetallic for hydrogen absorption. It has been reported, based on surface analysis and magnetic investigations [12, 13], that oxygen-induced surface segregation occurs with the formation of metallic nickel precipitates and this metallic subsurface could account for the high hydrogen uptake rate of many of the nickel-containing  $\text{AB}_5$ -type intermetallics. However, there is a contradictory report [14] that it is nickel, and not lanthanum, that is oxidized on the surface of the  $\text{LaNi}_5$  alloy. The present result, however, does not seem to support this model.

The charging effects observed in the core level emissions are slowly removed as a result of successive sputtering and this could be due to removal of the insulating oxide films covering the surface of the as-received sample. It is observed that the insulating  $\text{CaO}$  species persist even after sputtering to about 1000 sec while that of the nickel (oxygen) species could be removed in the initial stages of sputtering itself ( $\sim 160$  sec sputtering). This observation indicates that calcium in deep subsurface layers is oxidized while only the surface nickel species are oxidized and that too only to a partial extent. The presence of this persistent calcium oxide insulating layer could be the reason for the observed partial charging during photoemission experiments, thus resulting in the observation of the core level emission at higher binding energy values. This species could arise from the preferential oxidation of calcium which is a thermodynamically more favourable process compared to the oxidation of nickel ( $\Delta G_{298}^0(\text{CaO}) = -144.4 \text{ kcal mol}^{-1}$  and  $\Delta G_{298}^0(\text{NiO}) = -57.3 \text{ kcal mol}^{-1}$ ). If this postu-

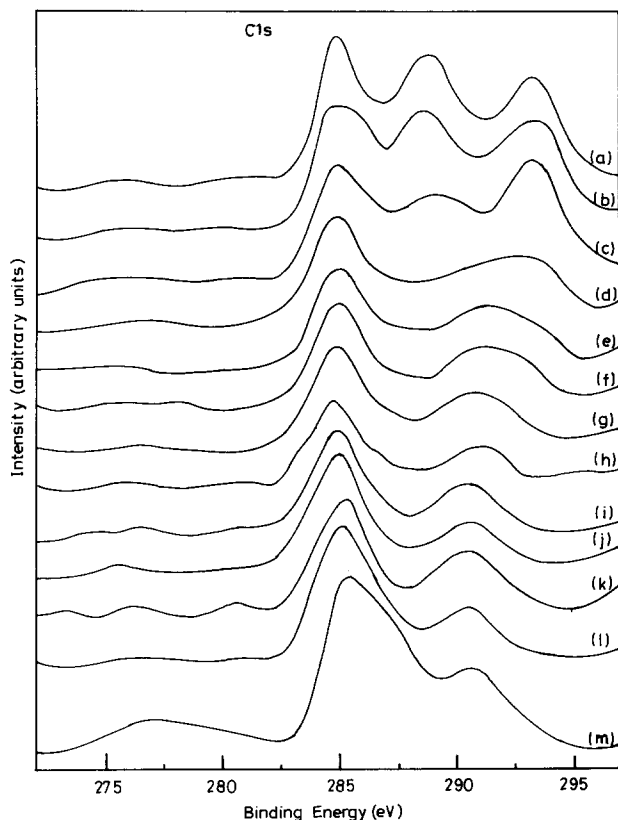


Figure 4 XPS (C 1s) spectra for the  $\text{CaNi}_5$  alloy; (a) to (m) as in Fig. 1.

late were to be true then one should observe the chemical reaction-induced segregation of calcium to the surface and subsurface layers.

In view of the above observations and in order to confirm the assumptions, a depth profile analysis of the air-exposed  $\text{CaNi}_5$  alloy was carried out as a function of sputtering time, monitoring the intensities of the XPS emission peaks. The data are presented in Fig. 5. It is seen that the Ca/Ni ratio is higher than the stoichiometry composition on the surface as well as in the subsurface layers and the value tends towards the theoretical value only after extensive sputtering of up to 7000 sec. This enrichment of calcium is due to oxygen-induced surface reaction as is evident from the rapid increase of Ca/O ratio in the initial stages of sputtering, while the Ni/O ratio increases at a much

slower rate in the initial stages of sputtering. However, at deep subsurface layers, the precipitated nickel clusters seem to be highly reactive towards oxygen compared to calcium. Therefore, the preferential segregation of calcium in the  $\text{CaNi}_5$  alloy is mainly due to induced surface segregation with oxygen which is a thermodynamically more favourable process. The contribution from other factors such as surface energy differences and other entropy factors could be negligible or small, compared to the reaction-induced segregation effects. This conclusion is further supported by the observation that more nickel is present in the uppermost layers of the surface than in the immediate subsurface layers, as can be seen from Fig. 5. The Ca/Ni ratio increases drastically with sputtering for a few minutes, though there is an initial decrease to a small extent. If the surface energy factor was to dominate in the segregation process, a look at the surface energies of calcium and nickel ( $\text{Ca} = 490 \text{ mJ m}^{-2}$  and  $\text{Ni} = 2450 \text{ mJ m}^{-2}$ ) indicates that there should be greater enrichment of calcium on the uppermost layers when compared to the subsurface layers, which is not true in the present case. A similar observation has been made for the  $\text{LaNi}_3\text{Mn}_2$  system [15] where the  $\text{La}/[\text{Ni} + \text{Mn}]$  ratio increases and then decreases on sputtering.

In view of the fact that the results obtained in the present study conform to the general pattern observed with other  $\text{AB}_5$ -type intermetallics, it is appropriate an attempt should be made to compare the behaviour of these systems, at least to a limited extent.

Weaver *et al.* [9] studied the valance bands of isomorphous Haucke compounds,  $\text{CaNi}_5$ ,  $\text{YNi}_5$ ,  $\text{LaNi}_5$  and  $\text{ThNi}_5$  and concluded that both the constituents are oxidized when exposed to oxygen and hence the differing hydrogenation characteristics of these compounds cannot be explained by either the differences in the electronic structures or the gettering effect of the non-nickel species which keeps nickel metallic. This is in contrast to the observation of Schlapbach and Brundle [6] who, as stated earlier, reported that the surface segregation in  $\text{LaNi}_5$  and  $\text{ThNi}_5$  is predominantly induced by the reaction of the A component with oxygen, and at low coverages of oxygen, nickel essentially remains metallic. The ternary system

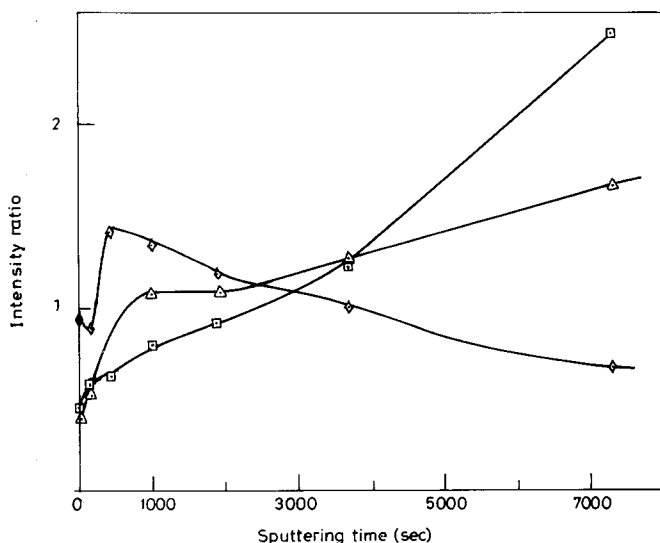


Figure 5 Relative elemental intensities on the surface plotted against sputtering time for the  $\text{CaNi}_5$  alloy. ( $\diamond$ )  $I_{\text{Ni}}/I_{\text{O}}$ , ( $\square$ )  $I_{\text{Ni}}/I_{\text{O}}$ , ( $\Delta$ )  $I_{\text{Ca}}/I_{\text{O}}$ .

LaNi<sub>3</sub>Mn<sub>2</sub> has been examined by Lartigue *et al.* [15]. They observed that the air-exposed sample is contaminated by oxygen and carbon. The top layers consist of mainly lanthanum hydroxide and manganese oxide while subsurface layers mainly consist of lanthanum oxide and metallic nickel. The surface segregation induced by oxygen easily occurs in LaNi<sub>3</sub>Mn<sub>2</sub>, with enrichment of lanthanum and manganese. Dang *et al.* [16] investigated a similar system, namely ThNi<sub>x</sub>Fe<sub>5-x</sub>, in which they report that the oxidized system is enriched in iron on the surface layers. The results obtained in the present study on the CaNi<sub>5</sub> system are thus in agreement with other reports in the literature on similar AB<sub>5</sub>-type systems.

CaNi<sub>5</sub> is different from the lanthanum-based alloys in some respects. In the CaNi<sub>5</sub> system, as is evident from the atomic ratios, the surface is relatively richer in nickel when compared to the surface of the LaNi<sub>5</sub> system. Also, on sputtering, an initial decrease in the Ca/Ni ratio is observed which later increases. Such a trend is not observed in the LaNi<sub>5</sub> system. CaNi<sub>5</sub> differs from the other AB<sub>5</sub> systems in one other aspect, i.e. the observation of a shift of 3 to 4 eV in the XPS emissions of all the peaks for the air-exposed sample due to partial charging. Such an observation has not been recorded with the other systems.

### Acknowledgements

We thank the CSIR, New Delhi for financial assistance to one of us (MPS). The authors also thank RSIC, IIT Madras for providing the facilities for XPS measurements.

### References

1. M. S. BAWA and E. A. ZIEM, *Int. J. Hydrogen Energy* **7** (1982) 775.
2. H. H. VAN MAL, *Philips Res. Repts. Suppl.* (1976) p. 1.
3. P. SELVAM, B. VISWANATHAN, C. S. SWAMY and V. SRINIVASAN, *Int. J. Hydrogen Energy* **11** (1986) 169.
4. J. J. REILLEY and R. H. WISWALL, *Inorg. Chem.* **13** (1974) 218.
5. *Idem.*, *ibid.* **7** (1968) 2254.
6. L. SCHLAPBACH, A. SEILER, F. STUCKI and H. C. SEIGMANN, *J. Less-Common Met.* **73** (1980) 145.
7. L. SCHLAPBACH and C. R. BRUNDLE, *J. Physique* **42** (1981) 1025.
8. L. SCHLAPBACH, *Solid State Commun* **38** (1981) 117.
9. J. H. WEAVER, A. FRANCIOSCI, D. J. PETERMAN, T. TAKESHITA and K. A. GSCHNEIDNER Jr, *J. Less-Common Met.* **86** (1982) 195.
10. H. VAN DOVEREN and J. A. Th. VERHOEVEN, *J. Electron Spectr. Rel. Phenom.* **21** (1980) 265.
11. W. N. DELGASS, T. R. HUGHES and C. S. FADLEY, *Catal. Rev.* **4** (1970) 179.
12. H. C. SIEGMANN, L. SCHLAPBACH and C. R. BRUNDLE, *Phys. Rev. Lett.* **40** (1978) 972.
13. L. SCHLAPBACH, A. SEILER, H. C. SEIGMANN, T. VON WALDKIRCH, P. ZURCHER and C. R. BRUNDLE, *Int. J. Hydrogen Energy* **4** (1978) 21.
14. J. H. WEAVER, A. FRANCIOSCI, W. E. WALLACE and H. K. SMITH, *J. Appl. Phys.* **51** (1980) 5847.
15. C. LARTIGUE, YU XIN-NAN, JIANG ZHAXO XUE, LIN ZHANG DA, A. PERCHERON-GUEGAN and J. C. ACHARD, *J. Less-Common Met.* **130** (1987) 517.
16. T. A. DANG, L. PETRAKIS and D. M. HERCULES, *J. Phys. Chem.* **88** (1984) 3209.

*Received 20 September 1988  
and accepted 24 February 1989*